

## Danggui Niantong granules ameliorate rheumatoid arthritis by regulating intestinal flora and promoting mitochondrial apoptosis

Qi-Jin Lu<sup>a\*</sup>, Jia-Yu Li<sup>b\*</sup>, Hong-Xin Lin<sup>a†</sup>, Yi-Si Cai<sup>a†</sup>, Chang-Shun Liu<sup>c,d</sup>, Li-Ping Fu<sup>e</sup>, Gang Liu<sup>e</sup> and Li-Xia Yuan<sup>c,d</sup>

<sup>a</sup>Traditional Chinese Pharmacological Laboratory, School of Traditional Chinese Medicine, Southern Medical University, Guangzhou, China; <sup>b</sup>School of Laboratory Medicine and Biotechnology, Southern Medical University, Guangzhou, China; <sup>c</sup>School of Traditional Chinese Medicine, Southern Medical University, Guangzhou, China; <sup>d</sup>Guangdong Provincial Key Laboratory of Chinese Medicine Pharmaceuticals, Southern Medical University, Guangzhou, China; <sup>e</sup>Nanfeng Hospital of Southern Medical University, Guangzhou, China

### ABSTRACT

**Context:** Danggui Niantong Granules (DGNTG) are a valid and reliable traditional herbal formula, commonly used in clinical practice to treat rheumatoid arthritis (RA). However, the mechanism of its effect on RA remains unclear.

**Objective:** An investigation of the therapeutic effects of DGNTG on RA.

**Materials and methods:** Twenty-four male Sprague-Dawley (SD) rats were divided into four groups: control, model, DGNTG (2.16 g/kg, gavage), methotrexate (MTX) (1.35 mg/kg, gavage) for 28 days. The morphology of synovial and ankle tissues was observed by haematoxylin-eosin staining. The responses of mitochondrial apoptosis were assessed by qPCR, Western blotting and immunohistochemical staining. Rat faeces were analysed by 16S rRNA sequencing.

**Results:** Our results showed that DGNTG treatment reduced AI scores ( $7.83 \pm 0.37$  vs.  $4.67 \pm 0.47$ ,  $p < 0.01$ ) and paw volumes ( $7.63 \pm 0.17$  vs.  $6.13 \pm 0.11$ ,  $p < 0.01$ ) compared with the model group. DGNTG also increased the expression of Bax ( $0.34 \pm 0.03$  vs.  $0.73 \pm 0.03$ ,  $p < 0.01$ ), cytochrome c (CYTC) ( $0.24 \pm 0.02$  vs.  $0.64 \pm 0.01$ ,  $p < 0.01$ ) and cleaved caspase-9 ( $0.24 \pm 0.04$  vs.  $0.83 \pm 0.08$ ,  $p < 0.01$ ), and decreased bcl-2 ( $1.70 \pm 0.11$  vs.  $0.60 \pm 0.09$ ,  $p < 0.01$ ) expression. DGNTG treatment regulated the structure of gut microbiota.

**Discussion and conclusions:** DGNTG ameliorated RA by promoting mitochondrial apoptosis, which may be associated with regulating gut microbiota structure. DGNTG can be used as a supplement and alternative drug for the treatment of RA; its ability to prevent RA deserves further study.

### ARTICLE HISTORY

Received 28 March 2022

Revised 5 July 2022

Accepted 25 July 2022

### KEYWORDS





Adjuvant-induced arthritis rats; fibroblast-like synovial cells; gut microbiota; traditional Chinese medicine

### Introduction

Rheumatoid arthritis (RA) is a systemic autoimmune disease that presents with chronic inflammatory lesions of the synovial tissue of the joints; its incidence in China is about  $0.5 \approx 1\%$  (Alamanos and Drosos 2005; Smolen et al. 2016). The clinical manifestations of RA are mainly erosive and symmetrical arthritis, even involving small joints, causing destruction of subchondral bone and osteoporosis, and resulting in bone and cartilage diseases (Aletaha and Smolen 2018). The typical pathological features of RA include over proliferation of synovial cells, deficiency of synovial cell apoptosis, secretion of high levels of proinflammatory factors and pannus formation (Feng and Qiu 2018; Ma et al. 2019), which are the main factors that contribute to the excessive proliferation and erosion of synovial tissue. Conventional drug therapies for RA are generally disease-relieving, but most cause serious adverse reactions, such as hepatotoxicity, gastrointestinal injury and blood abnormalities (Wang W et al. 2018). Fortunately, for the treatment of RA, traditional Chinese medicines (TCMs) have advantages of fewer side effects and lower cost.

Danggui Niantong Granules (DGNTGs) are a traditional and classical Chinese medicine processed by Danggui Niantong Decoction. DGNTG consist of 15 traditional Chinese herbs (Table 1). Studies have confirmed that DGNTG has a significant ameliorating effect on RA, which can reduce inflammation indicators, inhibit the progression of RA and reduce the occurrence of adverse reactions (Zhao et al. 2019). Most of the main active ingredients of DGNTG have been proven to have the effect of reducing symptoms in patients with RA. For example, baicalin and chlorogenic acid can suppress proliferation and induce apoptosis of fibroblast-like synovial cells (FLS) (Lou et al. 2016; Fu et al. 2019; Sun and Gu 2019). Our previous research found that DGNTG had a significant inhibitory effect on *in vitro* RA-FLS proliferation experiments (Zhao et al. 2020).

Apoptosis is a type of programmed cell death which is closely linked to autoimmune disorders. The pathological characteristics of RA include excessive synovial tissue hyperplasia, pannus formation and bone erosion, and the pathological basis of RA is generally considered excessive proliferation and insufficient apoptosis of FLS (Zhang Q et al. 2019). Thus, a combination of

**CONTACT** Gang Liu  [liugang0999@126.com](mailto:liugang0999@126.com)  Nanfeng Hospital of Southern Medical University, Guangzhou, China; Li-Xia Yuan  [cnylxtcm@163.com](mailto:cnylxtcm@163.com)  Guangdong Provincial Key Laboratory of Chinese Medicine Pharmaceuticals, Southern Medical University, Guangzhou, China

\*Qi-Jin Lu and Jia-Yu Li have contributed equally to this work and share the first authorship.

†Hong-Xin Lin and Yi-Si Cai have contributed equally to this work and share second authorship.

© 2022 The Author(s). Published by Informa UK Limited, trading as Taylor & Francis Group.

This is an Open Access article distributed under the terms of the Creative Commons Attribution-NonCommercial License (<http://creativecommons.org/licenses/by-nc/4.0/>), which permits unrestricted non-commercial use, distribution, and reproduction in any medium, provided the original work is properly cited.

**Table 1.** Composition of DGNTG.

Plant	Family	English name	Part of plant
<i>Artemisia capillaris</i> Thunb	Asteraceae	Artemisiae Scopariae Herba	whole plant
<i>Angelica sinensis</i> (Oliv.) Diels	Umbelliferae	Angelicae Sinensis Radix	root
<i>Notopterygium incisum</i> Ting ex H. T. Chang	Umbelliferae	Notopterygii Rhizoma et Radix	root
<i>Scutellaria baicalensis</i> Georgi	Lamiaceae	Scutellariae Radix	root
<i>Polyporus umbellatus</i>	Sargassaceae	Polyporus	whole plant
<i>Sophora flavescens</i> Alt	Leguminosae	Sophorae Flavescentis Radix	root
<i>Alisma plantago-aquatica</i> L	Alismaceae	Alismatis Rhizoma	tuber
<i>Anemarrhena asphodeloides</i> Bunge	Liliaceae	Anemarrhenae Rhizoma	rhizome
<i>Saposhnikovia divaricata</i> (Turcz.) Schischk.	Umbelliferae	Saposhnikoviae Radix	root
<i>Atractylodes lancea</i> (Thunb.) DC.	Asteraceae	Atractylodis Rhizoma	rhizome
Lobed Kudzuvine Root	Leguminosae	Puerariae Lobatae Radix	root
<i>Panax ginseng</i> C. A. Meyer	Araliaceae	Ginseng Radix et Rhizoma	root
<i>Glycyrrhiza uralensis</i> Fisch	Leguminosae	Glycyrrhizae Radix et Rhizoma	root and tuber
<i>Atractylodes macrocephala</i> Koidz	Asteraceae	Atractylodis Macrocephalae Rhizoma	tuber
<i>Cimicifuga foetida</i> L	Ranunculaceae	Cimicifugae Rhizoma	tuber

inhibition of FLS proliferation and the initiation of apoptosis is considered as an ideal approach for the treatment of RA. The process of apoptosis mainly includes the Fas-mediated extrinsic pathway and the Bcl-2/Bax-regulated intrinsic mitochondrial pathway. Members of the Bcl-2 protein family function as pro- and anti-apoptotic regulators. In recent years, studies have found that the intestinal flora, an important internal environmental factor, plays an increasingly important role in RA (Zaiss et al. 2021). Previous studies have reported that gut microbiota produced immunomodulatory and inflammatory effects in RA (du Teil Espina et al. 2019). Moreover, accumulating evidence has shown the role of gut microbiota in the regulating cell apoptosis. *Bifidobacterium* and *Bacteroides fragilis* inhibit cell apoptosis via multiple methods (Saito et al. 2019; Nie et al. 2020; Zhou et al. 2020). Thus, it is suggested that restoration of gut microbiota and regulation of mitochondrial apoptosis may be an effective approach for the treatment of RA.

Our previous study demonstrated that DGNTG treatment of RA may regulate the induction of apoptosis through the Fas/caspase-8 pathway (Zhao et al. 2020). Whether DGNTG treatment involves the modulation of mitochondrial apoptosis and gut microbial composition remains unclear. Therefore, in this study, we sought to investigate the effect of DGNTG on RA in adjuvant-induced arthritis (AA) rats. Moreover, the responses of mitochondrial apoptosis in the synovial tissue of AA rats were assessed. Furthermore, we explored whether DGNTG treatment of RA involved the modulation of gut microbiota. The correlation between key bacteria and mitochondrial apoptosis was analysed.

## Materials and methods

### Materials

*Mycobacterium tuberculosis* (Mtb), H37RA, was purchased from Becton, Dickinson and Company (NV, USA). Mineral oil was purchased from Sigma (MO, USA). Methotrexate (MTX) was purchased from Shanghai Sine Pharmaceutical Laboratories Co., Ltd (Shanghai, China). ChamQ SYBR qPCR Master Mix, HiScript® III RT SuperMix for qPCR (+gDNA wiper) and trizol were purchased from Nanjing Vazyme Biotech Co., Ltd (Nanjing, China). Primers for GAPDH, Bax, Bcl-2, cytochrome c and caspase-9 were purchased from Tsingke Biological Technology Co., Ltd (Beijing, China). Secondary antibody was purchased from Affinity (USA). Anti-caspase-9, anti-Bax, anti-Bcl-2 and anti-cytochrome c were purchased from Proteintech (USA). Anti-β-actin and anti-cleaved caspase-9 were purchased from Cell Signalling Technology (USA).

### Preparation and high-performance liquid chromatography (HPLC) analysis of DGNTG

DGNTG is composed of 15 Chinese medicinal herbs as shown in Table 1. DGNTG was provided by Jiangxi Xinglin Baima Pharmaceutical Co., Ltd (Jiangxi, China), batch number 2017B02868. To prepare the granules, 15 medicinal herbs were divided into four portions and extracted four times with distilled water by decoction, the extracts were filtered, mixed and dried to a powder. DGNTG was prepared from these powders and dextrin was added appropriately. Quality control of DGNTG was analysed by High Performance Liquid Chromatography (HPLC). DGNTG was diluted to obtain a final concentration of 4 mg/mL using methanol. The mixture was sonicated, centrifuged and filtered. Baicalin was used as a standard for identification of the components of DGNTG. HPLC was performed on an Agilent 1260 Infinity II System with Variable Wavelength Detector (VWD).

An Agilent C18 (4.6 mm × 250 mm, 5 μm) column was used for HPLC analyses. The flow rate was 1.0 mL/min and the injection volume was 10 μL. Samples were monitored by absorption at 280 nm. The mobile phase was methanol: 0.2% phosphoric acid (47:53). Preparation of the reference solution was as follows: an appropriate amount of baicalin standard was precisely weighed and added with methanol to a concentration of 60 μg/mL.

### Establishment of animal model

Twenty-four male Sprague-Dawley (SD) rats (6–8 weeks, 160 ± 20 g) were purchased from Experiment Animal Centre of Southern Medical University (Guangzhou, China). The experiments were approved by the Ethics Committee of Southern Medical University (No. L2019201). Male SD rats were housed under standard laboratory conditions at a temperature of 25 °C and relative humidity of 60%, with a 12-h light/dark cycle. Animal experiments were designed according to Zhang RX et al. (2009) with minor modifications. The entire experiment lasted for 28 days. On day 0, adjuvant arthritis (AA) was induced in rats by subcutaneous injection at the base of the tail of 0.2 mL of 5 mg/mL Complete Freund's Adjuvant (CFA) solution, which was prepared by suspending heat-killed *Mycobacterium tuberculosis* (Mtb) in mineral oil. After CFA injection, AA rats were divided into three groups at random ( $n = 6$ ): AA model (sterile water), DGNTG (2.16 g/kg) and methotrexate (MTX) (1.35 mg/kg). Normal rats served as the control group ( $n = 6$ ). The dose of DGNTG and MTX was determined with the following formula: animal equivalent dose (g/kg) = human dose

(g/kg)  $\times$   $K_m$  ratio (Nair and Jacob 2016). From day 0, DGNTG was given by gavage administration once a day for 28 days and MTX was divided in twice weekly. The control group and model group were given the same volume of distilled water.

### Collection of samples

After the 28 days of experimental period, samples were collected from the rats under anaesthesia. For synovial tissue isolation, the knee joints were cut open to expose the kneecap and the muscles. The ankles of rats were clipped; portions of the synovial tissue and all ankles were fixed in 4% paraformaldehyde and the remaining synovial tissue were stored at  $-80^\circ\text{C}$  for a follow-up experiment.

### Arthritis assessments

The rats were assessed every four days for signs of arthritis from day 0 to day 28. A well-established scoring system was used to measure the severity of arthritis in AA rats. Paws were graded according to severity and involvement site using a scale of 0 to 4 (Moudgil et al. 1997; Durai et al. 2004): 0, no redness or swelling; 1, redness and swelling of the toe joint; 2, redness and swelling of the toe joint and foot joint; 3, redness and swelling of the foot below the ankle joint; 4, all joints including the ankle joint were swollen and showed redness. The total score of both hind paws was 8. Paw volume was measured with a volume plethysmograph (Sichuan Keyicheng Technology Co., Ltd, China).

### Histopathological and histochemical detection

The synovial tissue and the knee joint were fixed in 4% paraformaldehyde, dehydrated and embedded in paraffin. The wax block was cut into  $4\ \mu\text{m}$  sections and stained with haematoxylin-eosin (HE).

Synovial tissue sections were dewaxed, rehydrated and antigens were repaired. Sections were then incubated overnight at  $4^\circ\text{C}$  with rabbit anti-Bax antibody, rabbit anti-Bcl-2 antibody or rabbit anti-Cytochrome c antibody. After washing with PBS, tissue was incubated with secondary antibodies for 2 h, and then incubated with DAB after washing with PBS again until the colour developed. The slides were washed with PBS and counterstained with haematoxylin. The slides were then sealed and observed using a microscope.

### Reverse transcription quantitative polymerase chain reaction (RT-qPCR)

Trizol reagent was used to extract total RNA from synovial tissue. NanoDropLite (Thermo Fisher Scientific, Waltham, MA, USA) was used to measure RNA concentration and purity. Then, the total RNA was reverse transcribed into cDNA using HiScript III RT SuperMix for qPCR (+gDNA wiper). The cDNAs were then used as templates for Vazyme Real-time PCR kit amplification. The cycle threshold (Ct) was recorded by the LightCycler96 system (Roche Applied Science, Penzberg, Germany) under the following reaction conditions:  $95^\circ\text{C}$  for 30 s, the 40 at  $95^\circ\text{C}$  for 10 s,  $60^\circ\text{C}$  for 30 s. Each qPCR run was assessed by the melting and cooling programs set by Roche's real-time fluorescent quantitative PCR instrument, and we used the  $2^{-\Delta\Delta\text{CT}}$  method to calculate the relative expression of mRNA. The primers were designed by the NCBI Primer-blast website and synthesized by

**Table 2.** The primer sequences used for real-time quantitative PCR.

Gene	Primer sequences (5'–3')	Length (bp)
GAPDH	Forward: GAACGGGAAGCTCACTGG Reverse: GCCTGCTTACCACCTTCT	123
Bax	Forward: AGCTGCAGAGGATGATTGCTG Reverse: CTGATCAGCTCGGGCACTTTA	178
Bcl-2	Forward: TGGCCTTCTTTGAGTTCGGT Reverse: GATGCCGGTTCAGTACTCA	111
Cytochrome c	Forward: CTTGGGCTAGAGAGCGGGA Reverse: CCATGGAGGTTTGGTCCAGT	179
Caspase-9	Forward: AGCTGGCCCACTGTGAATAC Reverse: GCTCCACCTCAGTCAACTC	243

Tsingke Bio-Tech Co., Ltd. GAPDH was used as the internal reference. The primer sequences are shown in Table 2.

### Western blot analysis of proteins

Synovial tissue was transferred to a 2-mL homogenization tube with  $500\ \mu\text{L}$  of RIPA lysate containing protease inhibitor and phosphatase inhibitor, and the samples were homogenized in a homogenizer three times at 70 Hz. After homogenization, the sample was lysed at  $4^\circ\text{C}$  for 30 min, centrifuged and the supernatant was collected. The BCA method was used to determine the protein concentration. Protein samples ( $40\ \mu\text{g}$ ) were separated 10% SDS-PAGE and transferred to polyvinylidene difluoride (PVDF) membranes, which were enclosed with 5% bovine serum albumin at room temperature for 2 h. The membrane was then incubated with the primary antibody (1:1,000) overnight at  $4^\circ\text{C}$ , and then the membrane was incubated with secondary antibody (1:6,000) at room temperature for 2 h. The densitometric analysis of Western blots was performed using Image J software.

### Intestinal flora analysis

Faeces samples were collected randomly from three rats in each group after the last dose and frozen at  $-80^\circ\text{C}$ . Intestinal microbial genomic DNA extraction was performed on faecal samples according to the DNA extraction kit instructions. The integrity and purity of genomic DNA were monitored by 1% agarose gel electrophoresis, whereas NanoDropOne was used to assess the concentration and purity of DNA. PCR amplification of the V3V4 region of genomic DNA and product electrophoresis detection were performed. The Gene Tools Analysis Software (Version 4.03.05.0, SynGene) was used to compare the concentration of PCR products, calculate the required volume of each sample and mix the PCR products of each group. An E.Z.N.A. Gel Extraction kit was used to recover PCR products in TE buffer. The NEBNext Ultra DNALibrary Prep kit for Illumina was used with the high-throughput sequencing platform Illumina Hiseq to construct the sequencing library (Guangdong MagiGene Technology Co., Ltd). Sequence analysis and species annotations were performed by bioinformatics analysis. OTU cluster analysis to obtain community composition and structure at different levels in each group, analysis of  $\alpha$  and  $\beta$  diversity between samples and Pearson correlations between microbiota and mitochondrial apoptosis were calculated using R software based on the OTUs.

### Statistical analysis

The data are presented as mean  $\pm$  SD. The data were analysed using SPSS (V22). Data between groups were assessed by

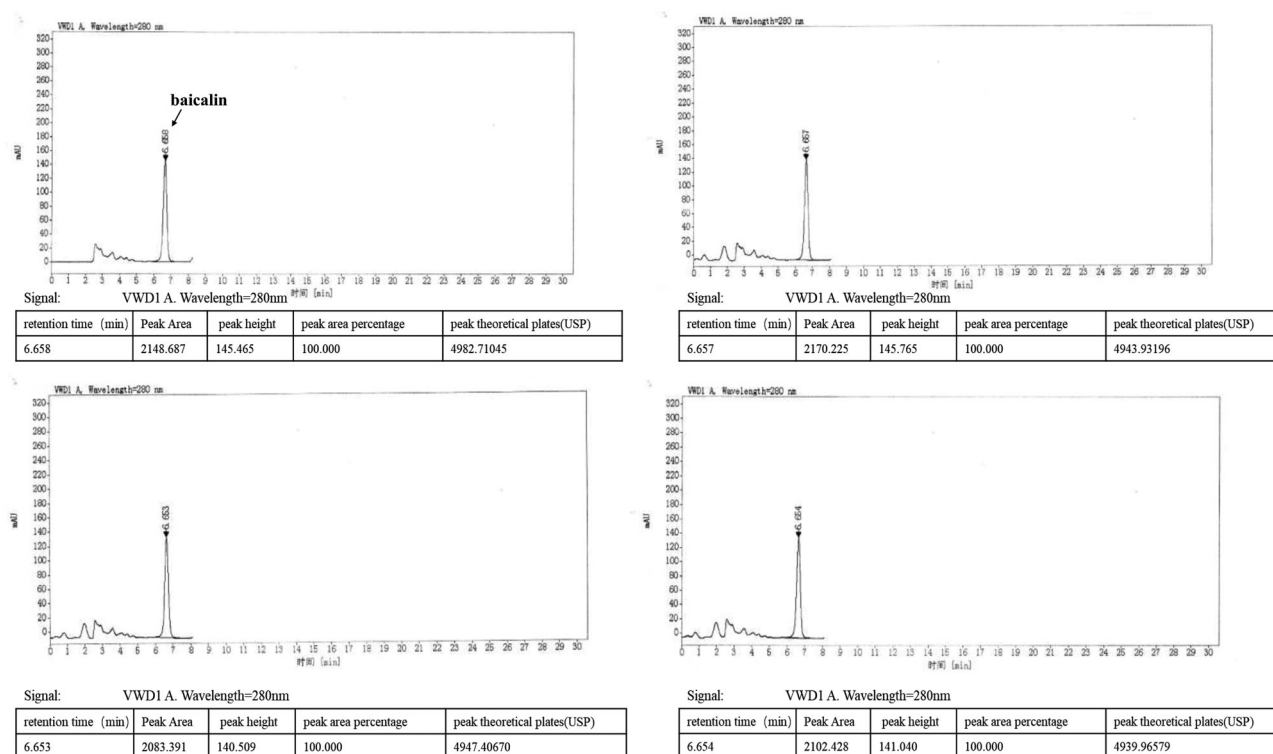


Figure 1. Quality control analysis of DGNTG by high performance liquid chromatography (HPLC).

Student's *t*-test analysis, analysis of variance or one-way ANOVA, followed by Tukey's post hoc test.  $p < 0.05$  was considered statistically significant.

## Results

### HPLC analysis of DGNTG

Quality control of DGNTG was performed using an HPLC system. The baicalin peak of DGNTG was determined by referencing the retention time of the baicalin standard. The results showed that the main component of DGNTG was baicalin (Figure 1).

### DGNTG treatment alleviated arthritis symptoms of AA rats

The effect of DGNTG on AA rats was assessed by histopathological changes in synovial tissue and ankle joints, body weight, paw volume and arthritis score. HE staining clearly revealed that the synovial tissues of the model group significantly proliferated, and were disordered in arranged, with a large number inflammatory cells present. These changes were reversed by DGNTG (2.16 g/kg/d) treatment (Figure 2(a)). AA rats exhibited obvious damaged articular surfaces, cartilage erosion, synovial hyperplasia and joint bone destruction. Our results showed that treatment of AA rats with DGNTG (2.16 g/kg/d) markedly attenuated the bone erosion and destruction of joints in AA rats (Figures 2(b)). Furthermore, the effects of DGNTG on body weight, paw volume and arthritis score were evaluated every four days during the whole experiment. As shown in Figure 2(c), compared with the control group, the growth rate of the rats in the model group was significantly slower, and the paw volume and arthritic scores were higher. Importantly, treatment with DGNTG greatly decreased the paw volume and arthritis score, and the rat body weights increased normally.

### DGNTG regulates the mRNA expression of mitochondrial apoptosis-related genes in AA rats

To validate whether the effect of DGNTG was associated with mitochondrial apoptosis, qRT-PCR was performed to analyse the mRNA levels of mitochondrial apoptosis-related genes, including Bcl-2-associated X (Bax), caspase-9, cytochrome c (CYTC), B-cell lymphoma factor (Bcl)-2. Compared with the control group, the mRNA expression levels of Bax, caspase-9 and CYTC were significantly decreased, whereas Bcl-2 was increased in the model group (Figure 3). However, DGNTG treatment reversed the mRNA levels of these genes.

### DGNTG modulates the protein expression of the mitochondrial apoptosis pathway in AA rats

We further detected changes in the expression of Bax, Bcl-2, CYTC, caspase-9 and cleaved caspase-9 by Western blot analysis (Figure 4(a)). DGNTG reduced the expression of Bcl-2, but promoted the expression of Bax, CYTC and cleaved caspase-9 compared with that in the model group (Figure 4(b)). As we expected, the immunohistochemical staining of Bax and CYTC was stronger in the rat synovial tissue of the DGNTG group compared with the model group. However, DGNTG treatment resulted in weak staining of Bcl-2 compared with the model group (Figure 4(c)).

### DGNTG regulates the composition of the gut microbiota in AA rats

To examine whether the alleviation of rheumatoid arthritis symptoms by DGNTG was related to gut microbiota, the bacterial 16S rRNA V3-V4 regions in faeces were sequenced. The results showed that there was no significant difference in the  $\alpha$

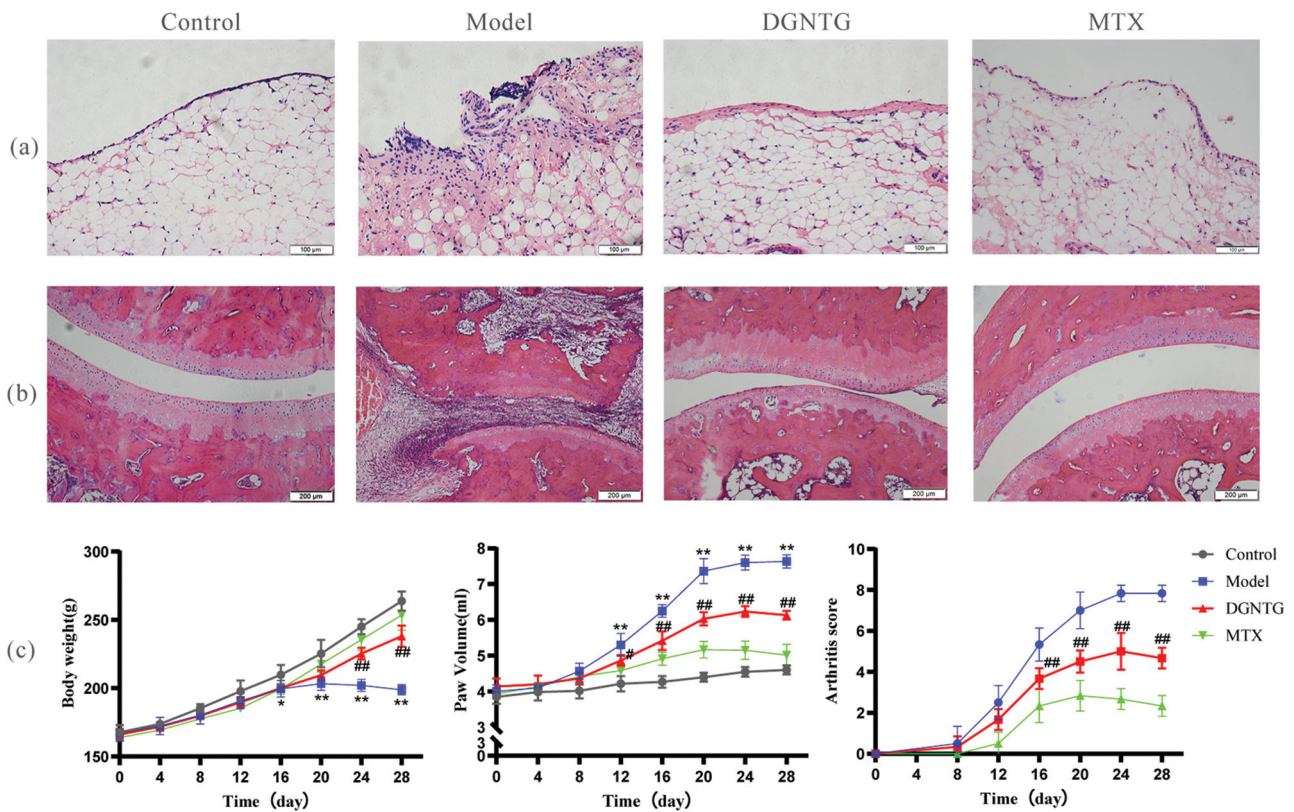


**Figure 2.** DGNTG ameliorates the severity of arthritis in rats. (a) HE staining of synovial tissue (200× magnification). (b) HE staining of ankle joints (100× magnification). (c) DGNTG impact on changes in body weight (left) and paw volume (middle) and arthritis score (right) in AA rats. Data are presented as the means ± SD.  $n = 6$ . \* $p < 0.05$  and \*\* $p < 0.01$  vs. control group, # $p < 0.05$  and ## $p < 0.01$  vs. model group.

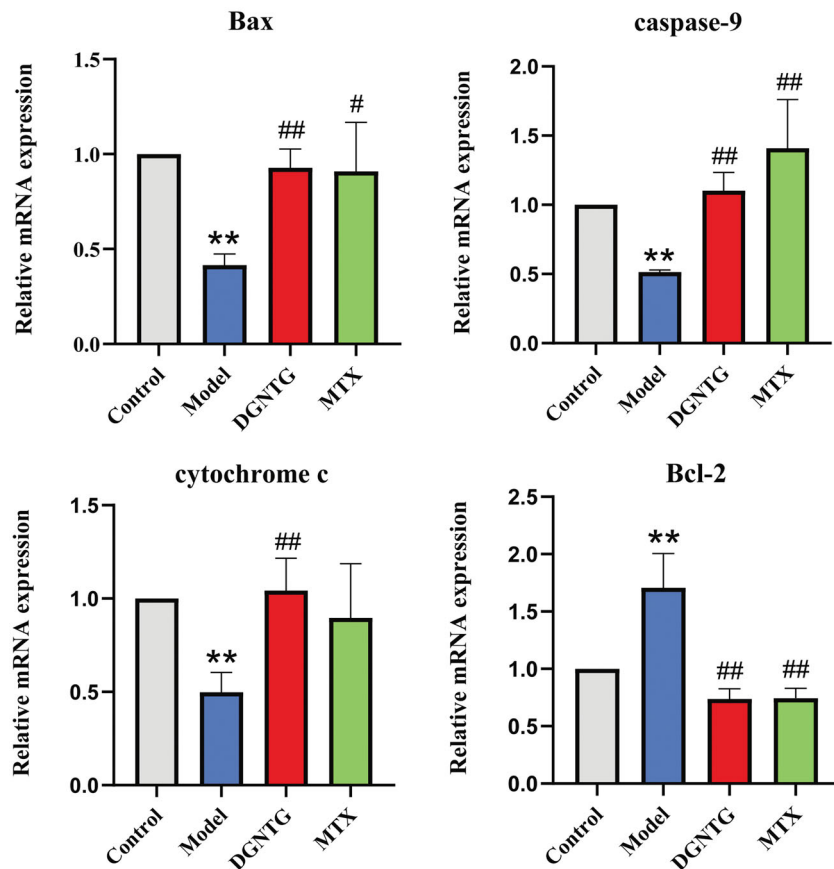


**Figure 3.** The effect of DGNTG on the mRNA levels of mitochondrial apoptosis-related genes in the synovial tissue of AA rats. Data are presented as the means ± SD.  $n = 3$ . \* $p < 0.05$  and \*\* $p < 0.01$  vs. control group, # $p < 0.05$  and ## $p < 0.01$  vs. model group.

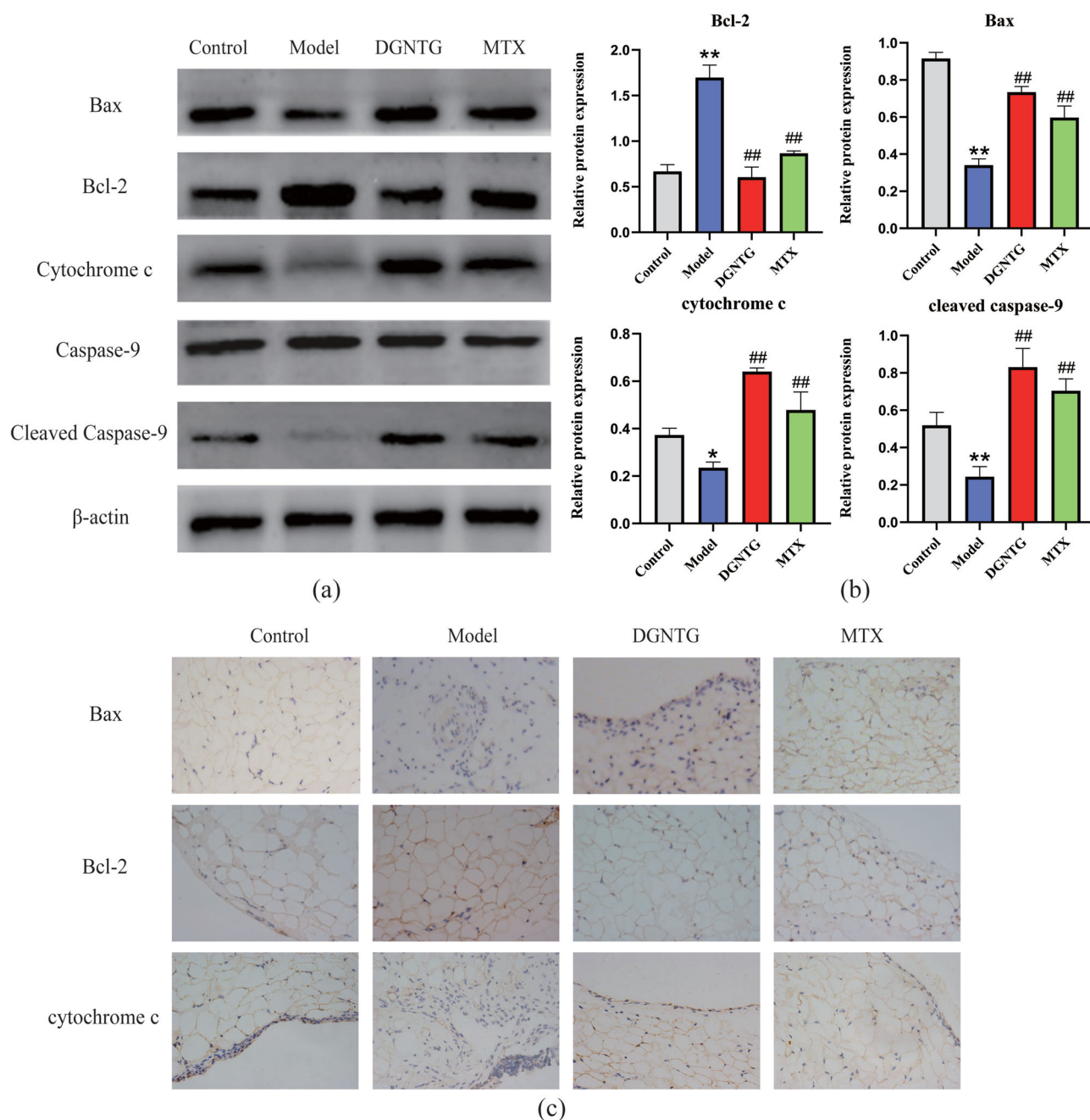


**Figure 4.** The effect of DGNTG on protein levels associated with mitochondrial apoptosis in rat synovial tissue. (a) Western blotting results of Bax, Bcl-2, cytochrome c, caspase-9, cleaved caspase-9 and  $\beta$ -actin in the synovial tissue of AA rats. (b) The relative expression of Bax, Bcl-2, cytochrome c and cleaved caspase-9 proteins. (c) Immunohistochemistry staining of Bax, Bcl-2, and cytochrome c of rat synovial tissue (400 $\times$  magnification). Data are presented as the means  $\pm$  SD.  $n = 3$ . \* $p < 0.05$  and \*\* $p < 0.01$  vs. control group, # $p < 0.05$  and ## $p < 0.01$  vs. model group.

diversity indices for Reads, Shannon and Simpson indices (Figure 5(a–c)).  $\beta$  Diversity was evaluated by principal component analysis (PCA) and principal coordinate analysis (PCoA), which clearly distinguished the control and model groups (Figure 5(d,e)). These results suggested that gut microbiota structure changed in the AA rats.

The microbiota composition of each group differed at the phylum, family and genus levels (Figure 6(a)). In all groups, Firmicutes and Bacteroidetes showed the highest relative abundance at the phylum level. In the model group, the ratio of Firmicutes to Bacteroidetes was significantly lower than that in the control group. Administration of DGNTG reversed these

changes by increasing the abundance of Firmicutes and decreasing the abundance of Bacteroidetes (Figure 6(b–d)). At the family level, DGNTG decreased the relative abundance of Muribaculaceae and increased the abundance of Lachnospiraceae (Figure 6(e,f)). At the genus level, there was no significant regulation of microbiota composition by DGNTG.

To explore the relationship between mitochondrial apoptosis and the gut microbiota, Pearson correlation was employed. We found *Prevotella*, *Lachnospiraceae\_NK4A136*, *Alloprevotella* and *Ruminiclostridium* were positively associated with Bax, Bcl-2 and CYTC, whereas *Ruminiclostridium*, *Christensenellaceae*, and

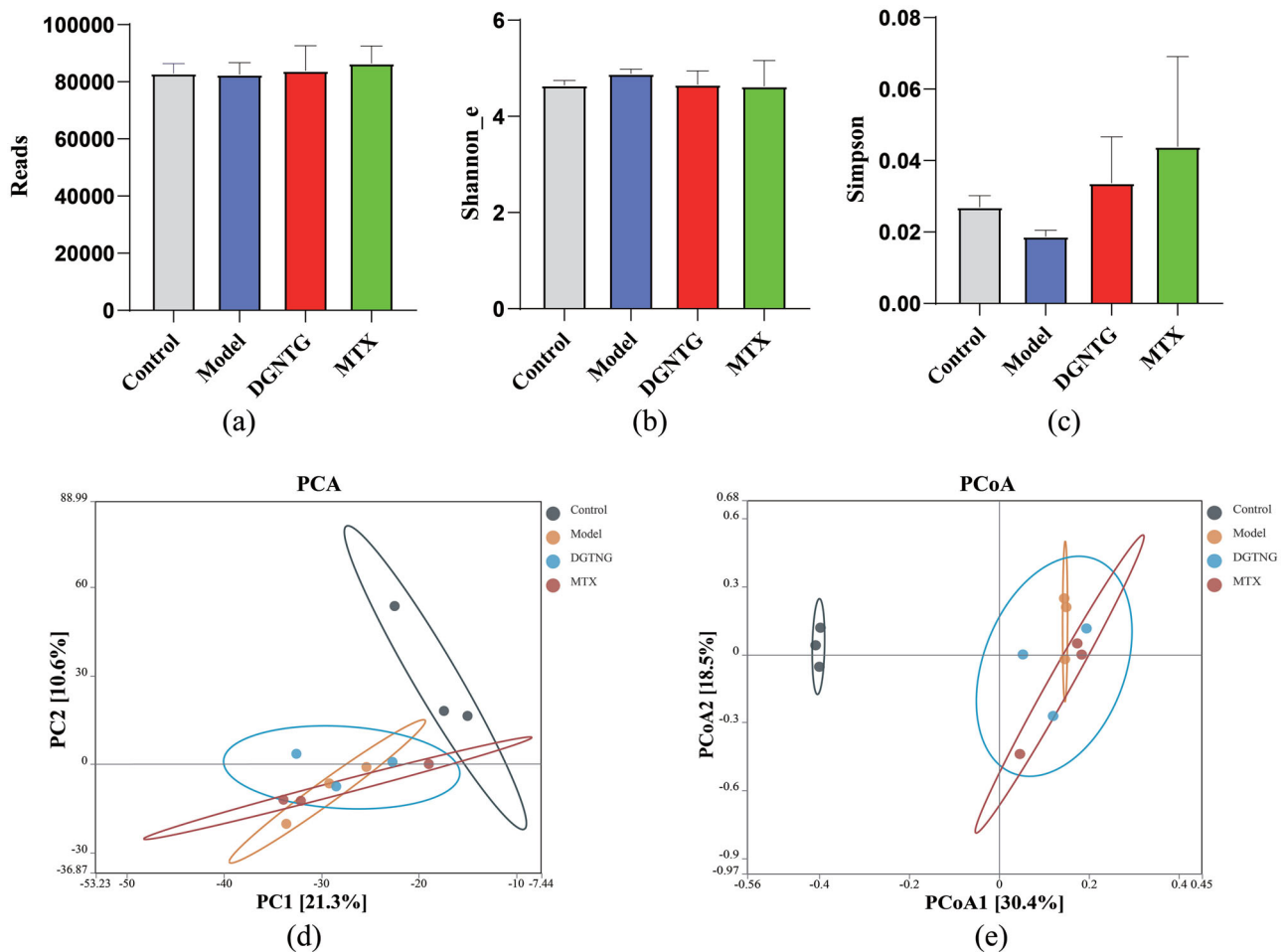


**Figure 5.** DGNTG regulates the structure of gut microbiota in AA rats. Alpha-diversity analysis by Reads index (a), Shannon\_e index (b) and Simpson index (c). Principal component analysis (PCA) of gut microbiota of rats among the control, model and DGNTG groups (d). Principal Coordinate Analysis (PCoA) of gut microbiota based on unweighted UniFrac (e). Data are presented as the means  $\pm$  SD.  $n = 3$ . \* $p < 0.05$  and \*\* $p < 0.01$  vs. control group, # $p < 0.05$  and ## $p < 0.01$  vs. model group.

*Bacteroides* had negative correlations with Bax and CYTC (Figure 7). The above results demonstrate that DGNTG modulates gut microbiota composition and the alterations in gut flora may be related to cell apoptosis.

## Discussion

This study was conducted to assess the effects of DGNTG on AA rats. Our results demonstrate a significant effect of DGNTG on RA, evinced by a reduction in excessive synovial tissue hyperplasia, joint inflammation, bone erosion, paw swelling and arthritis index of DGNTG-treated AA rats. We also showed that DGNTG regulated the mitochondrial apoptosis pathway and the changes of gut microbiota composition might be associated with the effects of DGNTG on mitochondrial apoptosis. DGNTG treatment, which is primarily aimed at preventing the development of RA, was initiated at the time of arthritis induction. The over proliferation of the synovial tissue expands and destroys the underlying cartilage and bone, leading to irreversible erosion of the bone in advanced stages of RA, which poses difficulties in treatment. Thus, our methodology focussed on intervention at early stages of the disease to prevent progression rather than after the disease was well established. The results suggested that DGNTG played an important role in RA prevention.

Mitochondria-mediated intrinsic apoptotic pathways are one of the important routes for cell apoptosis, and the mitochondrial apoptotic pathways are activated in response to mitochondrial damage, which is caused by a number of stress-induced conditions. In this study, DGNTG treatment increased the expressions of Bax, cytochrome c (CYTC) and cleaved caspase-9, but decreased the expression of Bcl-2. Bcl-2 and Bax, members of the Bcl family, have been identified as the main regulators of the mitochondrial pathways of apoptosis. The mechanism of these genes in the mitochondrial apoptotic pathway is as follows: (1) under the stimulation of apoptotic signals, the proapoptotic protein Bax is upregulated and activated, whereas the antiapoptotic protein Bcl-2 is downregulated; (2) the breaking of the balance between pro-/anti-apoptotic proteins results in changes in the permeability of the mitochondrial membrane, which leads to the release of CYTC; (3) released CYTC and caspase-9 form an 'apoptosome', which eventually activates the caspase cascade, which includes cleaved caspase-9 (Estaquier et al. 2012). In our study, we found that the model group had the lowest expression of Bax, CYTC, and cleaved caspase-9 compared with the control and DGNTG groups in AA rats. In addition, the antiapoptotic protein Bcl-2 was also altered accordingly. These results indicate that over-proliferation of synovial tissue in AA rats might be associated with insufficient apoptosis. After DGNTG treatment, the expression of the antiapoptotic protein Bcl-2 decreased, and the expression of proapoptotic proteins Bax, CYTC and cleaved

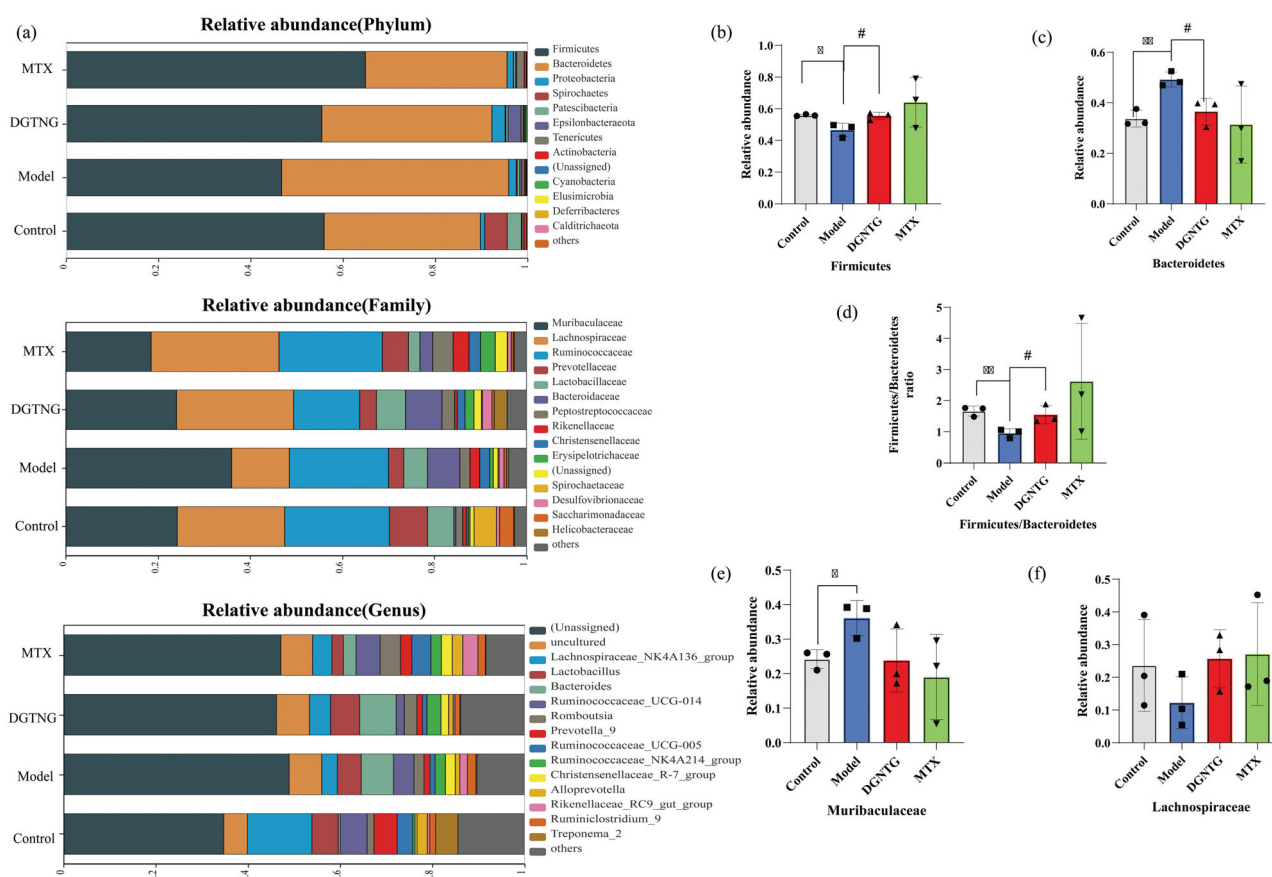


**Figure 6.** Relative abundance of the gut microbiota structure at the phylum, family and genus levels. The relative abundance of gut microbiota at the phylum, family and genus levels (a). The relative abundance of different bacteria at the phylum and family level (b–f). Data are presented as the means  $\pm$  SD.  $n = 3$ . \* $p < 0.05$  and \*\* $p < 0.01$  vs. control group, # $p < 0.05$  and ## $p < 0.01$  vs. model group.

caspase-9 increased in synovial tissue. The data we have presented suggest that the mitochondrial apoptosis pathway was involved in DGNTG-induced apoptosis of synovial tissue. As natural products, Chinese herbal medicines and their active ingredients are considered effective in treatment for RA due to their compelling efficacy. As the bioactive constituents of DGNTG, baicalin was previously shown to induce apoptosis by decreasing Bcl-2 levels, then activating Bax and caspase-9, which suggested that the mitochondrial pathway was involved in baicalin-induced apoptosis (Shu et al. 2014; Wan and Ouyang 2018). Therefore, promoting the death of FLS might be a feasible method for treating RA, and compared with other approaches, targeting FLS might ameliorate symptoms in patients with RA without systemic immune suppression (Zhang Q et al. 2019).

Recently, studies have demonstrated that the gut microbiota plays a key role in RA and microbiota are involved in RA pathogenesis (Asquith et al. 2019; Wang and Xu 2019). The gut flora was examined by 16S rRNA sequence analysis, which revealed the composition of intestinal microbiota. PCA and PCoA analysis showed that the model group was distinguished from the control group, suggesting that gut microbial composition was altered in AA rats. This result is consistent with human studies which revealed that patients with RA show significant differences in the gut microbiota compared with healthy controls (Zhong et al. 2018). After treatment with DGNTG, the alpha diversity (Simpson diversity) improved, and PCA and PCoA analyses revealed a more proximate distance between the DGNTG and control groups, but the differences were not significant. This

may be explained by the following: (1) the microbial communities were complex and had powerful abilities of self-repair, which would be consistent with a previous study that reported intestinal flora can maintain and repair their populations via self-replication (Backhed et al. 2005); (2) the main regulation of DGNTG on gut microbiota is to change the relative abundance of gut flora, not diversity. Overall, DGNTG treatment had little effect on the species diversity of gut microbiota in AA rats, even though DGNTG treatment significantly improved the arthritis symptoms of AA rats, indicating that the therapeutic effects of DGNTG may not rely on the diversity of gut microbiota.

Further investigation of the composition of intestinal flora showed *Bacteroidetes*, *Muribaculaceae* and *Bacteroides* were enriched, and the abundance of *Firmicutes* and *Lachnospiraceae* were diminished in the model group faecal samples. DGNTG increased the abundance of *Firmicutes* and decreased *Bacteroidetes*, suggesting DGNTG regulated the composition of the gut microbiota. A recent study found that *Firmicutes* were significantly decreased, whereas *Bacteroidetes* were increased, in CIA mice. The alteration of *Firmicutes* and *Bacteroidetes* during the priming phase of the immune response could cause an inflammatory response in the joints (Rogier et al. 2017; Nemoto et al. 2020). In our study, DGNTG increased the *Firmicutes/Bacteroidetes* ratio, which indicated DGNTG modulates the abundance of gut microbiota related to immunity and inflammation. Moreover, it has been reported that there was an increase in *Bacteroides* and a decrease in *Lactobacillus* and *Alloprevotella* in RA patients (Sun Y et al. 2019), and most treatments with



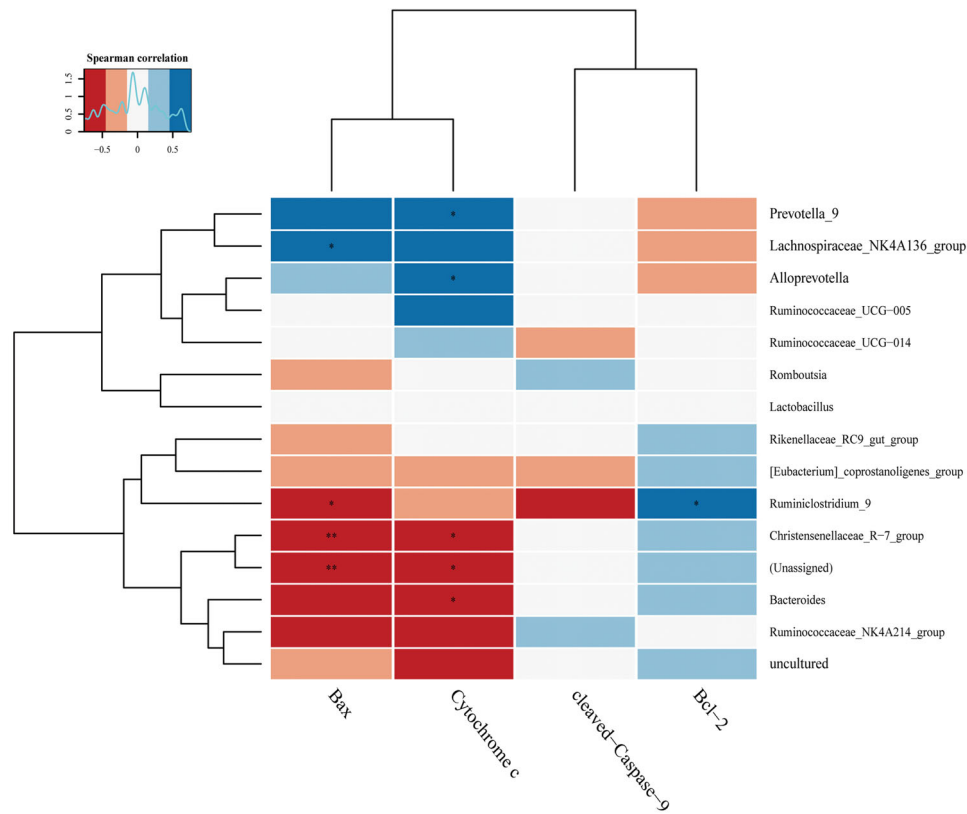


**Figure 7.** Heatmap of correlations between mitochondrial apoptosis and gut microbiota in the top 15 genera samples. (\*, \*\*) indicates a significant correlation ( $p < 0.05$ ,  $p < 0.01$ ). Correlation was determined by the Pearson correlation index.

these gut flora ameliorated RA symptoms through modulating the immune response and inflammatory cytokines (Horta-Baas et al. 2017; Larsen 2017). *Prevotella* may cross-react with self-epitopes of highly expressed proteins in joints and drive Th17 immune responses *in vitro* (de Aquino et al. 2014). *Lachnospiraceae* are associated with the regulation of inflammation (Xiao et al. 2018). In general, DGNTG reshaped the intestinal flora and primarily modulated the abundance of *Firmicutes*, *Bacteroidetes*, *Lachnospiraceae* and *Muribaculaceae*, indicating that the anti-arthritis effect of DGNTG involves intestinal microbiota.

Our correlation analysis indicated that DGNTG modulates gut microbiota, which may play a role in regulating mitochondrial apoptosis and improving RA. In recent reports, apoptosis was shown to be regulated at several levels, including the gut microbiota. For example, enterotoxins produced by *Bacteroides* can suppress apoptosis by regulating the MAPK pathway (Ko et al. 2016; Jeon et al. 2020). Some metabolites such as butyrate and propionate produced by *Firmicutes* and *Bacteroidetes* are correlated with apoptosis. Butyrate promotes cell growth through promoting proliferation as well as apoptosis inhibition, and propionate was reported to induce apoptosis by increasing expression of mitochondrial apoptotic pathway-related proteins (Kim et al. 2019; Mathew et al. 2019). DGNTG increased the abundance of *Firmicutes* and decreased the levels of *Bacteroidetes*, which indicate DGNTG modulates the abundance of intestinal flora related to apoptosis. Moreover, we found *Bacteroides* was negatively associated with CYTC and Bax, which might be related to reduced levels of apoptosis in the model group. Based on our results, we speculate that DGNTG promoted apoptosis, which may relate to regulation of the structure of intestinal flora.

However, we did not offer more direct evidence as to how DGNTG alleviates arthritis by regulating intestinal flora and which bacteria directly contribute to the anti-arthritis effect or contribute to the regulation of mitochondria-mediated intrinsic apoptotic pathways. Further study utilizing metabonomic analysis of intestinal flora may give us more insight into the mechanism of intestinal flora regulating apoptosis in RA.

## Conclusion

Our study showed that DGNTG improved the structure of gut microbiota, promoted mitochondrial apoptosis and ameliorated arthritis symptoms in RA, which might be associated with gut microbiota. These findings have improved our understanding of the mechanism underlying the impact of DGNTG on RA in terms of mitochondrial apoptosis and gut microbiota.

## Consent for publication

All named authors have agreed to the publication of this work.

## Author contributions

LiXia Yuan, QiJin Lu and JiaYu Li designed the study. LiPing Fu collected and integrated the data. QiJin Lu analysed the data and drafted the manuscript. Gang Liu revised the manuscript. HongXin Lin and YiSi Cai participated in the experiments. ChangShun Liu provided technical support. LiXia Yuan and Gang Liu handled the funding. All authors read and approved the final manuscript.

## Disclosure statement

No potential conflict of interest was reported by the author(s).

## Funding

This work was supported by the Natural Science Foundation of Guangdong Province [grant number 2022A1515011681], Natural Science Foundation of China (NSFC) [grant number 8167151349] and Natural Science Foundation of China (NSFC) [grant number 8177150993].

## Data availability statement

All data used to support the findings of this study are available within the article, or from the corresponding author upon reasonable request.

## References

- Alamanos Y, Drosos AA. 2005. Epidemiology of adult rheumatoid arthritis. *Autoimmun Rev.* 4(3):130–136.
- Aletaha D, Smolen JS. 2018. Diagnosis and management of rheumatoid arthritis: a review. *JAMA.* 320(13):1360–1372.
- Asquith M, Sternes PR, Costello ME, Karstens L, Diamond S, Martin TM, Li Z, Marshall MS, Spector TD, le Cao KA, et al. 2019. HLA Alleles associated with risk of ankylosing spondylitis and rheumatoid arthritis influence the gut microbiome. *Arthritis Rheumatol.* 71(10):1642–1650.
- Backhed F, Ley RE, Sonnenburg JL, Peterson DA, Gordon JI. 2005. Host-bacterial mutualism in the human intestine. *Science.* 307(5717):1915–1920.
- de Aquino SG, Abdollahi-Roodsaz S, Koenders MI, van de Loo FA, Pruijn GJ, Marijnissen RJ, Walgreen B, Helsen MM, van den Bersselaar LA, de Molon RS, et al. 2014. Periodontal pathogens directly promote autoimmune experimental arthritis by inducing a TLR2- and IL-1-driven Th17 response. *J Immunol.* 192(9):4103–4111.
- du Teil Espina M, Gabarrini G, Harmsen HJM, Westra J, van Winkelhoff AJ, van Dijk JM. 2019. Talk to your gut: the oral-gut microbiome axis and its immunomodulatory role in the etiology of rheumatoid arthritis. *FEMS Microbiol Rev.* 43(1):1–18.
- Durai M, Kim HR, Moudgil KD. 2004. The regulatory C-terminal determinants within mycobacterial heat shock protein 65 are cryptic and cross-reactive with the dominant self homologs: implications for the pathogenesis of autoimmune arthritis. *J Immunol.* 173(1):181–188.
- Estaquier J, Vallette F, Vayssiere JL, Mignotte B. 2012. The mitochondrial pathways of apoptosis. *Adv Exp Med Biol.* 942:157–183.
- Feng FB, Qiu HY. 2018. Effects of Artesunate on chondrocyte proliferation, apoptosis and autophagy through the PI3K/AKT/mTOR signaling pathway in rat models with rheumatoid arthritis. *Biomed Pharmacother.* 102:1209–1220.
- Fu X, Lyu X, Liu H, Zhong D, Xu Z, He F, Huang G. 2019. Chlorogenic acid inhibits BAFF expression in collagen-induced arthritis and human synovial cell MH7A cells by modulating the activation of the NF-kappaB signaling pathway. *J Immunol Res.* 2019:8042097.
- Horta-Baas G, Romero-Figueroa MDS, Montiel-Jarquín AJ, Pizano-Zarate ML, Garcia-Mena J, Ramirez-Duran N. 2017. Intestinal dysbiosis and rheumatoid arthritis: a link between gut microbiota and the pathogenesis of rheumatoid arthritis. *J Immunol Res.* 2017:4835189.
- Jeon JI, Choi JH, Lee KH, Kim JM. 2020. *Bacteroides fragilis* enterotoxin induces sulfiredoxin-1 expression in intestinal epithelial cell lines through a mitogen-activated protein kinases- and Nrf2-dependent pathway, leading to the suppression of apoptosis. *IJMS.* 21(15):5383.
- Kim K, Kwon O, Ryu TY, Jung CR, Kim J, Min JK, Kim DS, Son MY, Cho HS. 2019. Propionate of a microbiota metabolite induces cell apoptosis and cell cycle arrest in lung cancer. *Mol Med Rep.* 20(2):1569–1574.
- Ko SH, Rho da J, Jeon JI, Kim YJ, Woo HA, Lee YK, Kim JM. 2016. *Bacteroides fragilis* enterotoxin upregulates heme oxygenase-1 in intestinal epithelial cells via a mitogen-activated protein kinase- and NF-kappaB-dependent pathway, leading to modulation of apoptosis. *Infect Immun.* 84(9):2541–2554.
- Larsen JM. 2017. The immune response to *Prevotella* bacteria in chronic inflammatory disease. *Immunology.* 151(4):363–374.
- Lou L, Zhou J, Liu Y, Wei YI, Zhao J, Deng J, Dong B, Zhu L, Wu A, Yang Y, et al. 2016. Chlorogenic acid induces apoptosis to inhibit inflammatory proliferation of IL-6-induced fibroblast-like synoviocytes through modulating the activation of JAK/STAT and NF-kappaB signaling pathways. *Exp Ther Med.* 11(5):2054–2060.
- Ma C, Chen J, Li P. 2019. Geldanamycin induces apoptosis and inhibits inflammation in fibroblast-like synoviocytes isolated from rheumatoid arthritis patients. *J Cell Biochem.* 120(9):16254–16263.
- Mathew OP, Ranganna K, Mathew J, Zhu M, Yousefipour Z, Selvam C, Milton SG. 2019. Cellular effects of butyrate on vascular smooth muscle cells are mediated through disparate actions on dual targets, histone deacetylase (HDAC) activity and PI3K/Akt signaling network. *IJMS.* 20(12):2902.
- Moudgil KD, Chang TT, Eradat H, Chen AM, Gupta RS, Brahn E, Sercarz EE. 1997. Diversification of T cell responses to carboxy-terminal determinants within the 65-kD heat-shock protein is involved in regulation of autoimmune arthritis. *J Exp Med.* 185(7):1307–1316.
- Nair AB, Jacob S. 2016. A simple practice guide for dose conversion between animals and human. *J Basic Clin Pharm.* 7(2):27–31.
- Nemoto N, Takeda Y, Nara H, Araki A, Gazi MY, Takakubo Y, Naganuma Y, Takagi M, Asao H. 2020. Analysis of intestinal immunity and flora in a collagen-induced mouse arthritis model: differences during arthritis progression. *Int Immunol.* 32(1):49–56.
- Nie N, Bai C, Song S, Zhang Y, Wang B, Li Z. 2020. Bifidobacterium plays a protective role in TNF-alpha-induced inflammatory response in Caco-2 cell through NF-kappaB and p38MAPK pathways. *Mol Cell Biochem.* 464(1–2):83–91.
- Rogier R, Evans-Marin H, Manasson J, van der Kraan PM, Walgreen B, Helsen MM, van den Bersselaar LA, van de Loo FA, van Lent PL, Abramson SB, et al. 2017. Alteration of the intestinal microbiome characterizes preclinical inflammatory arthritis in mice and its modulation attenuates established arthritis. *Sci Rep.* 7(1):15613.
- Saito K, Suzuki R, Koyanagi Y, Isogai H, Yoneyama H, Isogai E. 2019. Inhibition of enterohemorrhagic *Escherichia coli* O157:H7 infection in a gnotobiotic mouse model with pre-colonization by *Bacteroides* strains. *Biomed Rep.* 10:175–182.
- Shu YJ, Bao RF, Wu XS, Weng H, Ding Q, Cao Y, Li ML, Mu JS, Wu WG, Ding QC, et al. 2014. Baicalin induces apoptosis of gallbladder carcinoma cells *in vitro* via a mitochondrial-mediated pathway and suppresses tumor growth *in vivo*. *Anticancer Agents Med Chem.* 14(8):1136–1145.
- Smolen JS, Aletaha D, McInnes IB. 2016. Rheumatoid arthritis. *Lancet (London, England).* 388(10055):2023–2038.
- Sun Y, Chen Q, Lin P, Xu R, He D, Ji W, Bian Y, Shen Y, Li Q, Liu C, et al. 2019. Characteristics of gut microbiota in patients with rheumatoid arthritis in Shanghai, China. *Front Cell Infect Microbiol.* 9:369.
- Sun F, Gu W. 2019. Baicalin attenuates collagen-induced arthritis via inhibition of JAK2-STAT3 signaling and regulation of Th17 cells in mice. *J Cell Commun Signal.* 13(1):65–73.
- Wan D, Ouyang H. 2018. Baicalin induces apoptosis in human osteosarcoma cell through ROS-mediated mitochondrial pathway. *Nat Prod Res.* 32(16):1996–2000.
- Wang W, Zhou H, Liu L. 2018. Side effects of methotrexate therapy for rheumatoid arthritis: a systematic review. *Eur J Med Chem.* 158:502–516.
- Wang Q, Xu R. 2019. Data-driven multiple-level analysis of gut-microbiome-immune-joint interactions in rheumatoid arthritis. *BMC Genomics.* 20(1):124.
- Xiao M, Fu X, Ni Y, Chen J, Jian S, Wang L, Li L, Du G. 2018. Protective effects of *Paederia scandens* extract on rheumatoid arthritis mouse model by modulating gut microbiota. *J Ethnopharmacol.* 226:97–104.
- Zaiss MM, Joyce Wu HJ, Mauro D, Schett G, Ciccia F. 2021. The gut-joint axis in rheumatoid arthritis. *Nat Rev Rheumatol.* 17(4):224–237.
- Zhang Q, Liu J, Zhang M, Wei S, Li R, Gao Y, Peng W, Wu C. 2019. Apoptosis induction of fibroblast-like synoviocytes is an important molecular-mechanism for herbal medicine along with its active components in treating rheumatoid arthritis. *Biomolecules.* 9(12):795.
- Zhang RX, Fan AY, Zhou AN, Moudgil KD, Ma ZZ, Lee DY, Fong HH, Berman BM, Lao L. 2009. Extract of the Chinese herbal formula Huo Luo Xiao Ling Dan inhibited adjuvant arthritis in rats. *J Ethnopharmacol.* 121(3):366–371.
- Zhao F, Li J, Lu Q, Chen E, Yuan L. 2020. [Danggui Niantong decoction induces apoptosis by activating Fas/caspase-8 pathway in rheumatoid arthritis fibroblast-like synoviocytes]. *Nan Fang Yi Ke Da Xue Xue Bao.* 40(8):1119–1126. Chinese.
- Zhao H, Zhou Z, Li J, Huang J, Cheng Y, Lu Z. 2019. [Clinical observation of addition and subtraction therapy and external washing treatment of Danggui Niantong decoction to knee osteoarthritis with heumatism heat bi syndrome]. *China J Exper Trad Med Formulae.* 25:105–110. Chinese
- Zhong D, Wu C, Zeng X, Wang Q. 2018. The role of gut microbiota in the pathogenesis of rheumatic diseases. *Clin Rheumatol.* 37(1):25–34.
- Zhou W, Cheng Y, Zhu P, Nasser MI, Zhang X, Zhao M. 2020. Implication of gut microbiota in cardiovascular diseases. *Oxid Med Cell Longev.* 2020:5394096.